

Ledford Sarah Holderness (Orcid ID: 0000-0003-1802-1961)

Title Page

Title: Downstream evolution of wastewater treatment plant nutrient signals using high-temporal monitoring

Running title: Downstream change in WWTP nutrient signal

Authors: Sarah H. Ledford* and Laura Toran

Institutional affiliation where work was conducted: Temple University, Department of Earth and Environmental Science, Philadelphia, PA

Acknowledgements: This work was funded by the William Penn Foundation as part of the Delaware River Watershed Initiative grant to Temple University. The authors thank Chelsea Kanaley for her assistance with field work.

Conflict of Interest Statement

The authors have no conflicts of interest to declare.

Data Availability

The data that support the findings of this study are openly available on CUAHSI's HydroShare database at <https://doi.org/10.4211/hs.7b81ceca6a5b426dac9905541fe27d95>

*Now at Georgia State University, Department of Geosciences, Atlanta, GA, sledford@gsu.edu

This article has been accepted for publication and undergone full peer review but has not been through the copyediting, typesetting, pagination and proofreading process which may lead to differences between this version and the Version of Record. Please cite this article as doi: 10.1002/hyp.13640

Title: Downstream evolution of wastewater treatment plant nutrient signals using high-temporal monitoring

Abstract: Wastewater treatment plants are major point-sources of nutrients to streams globally, but the impact on receiving streams is not always clear. Previous research has shown mixed responses in receiving streams, with some showing no net retention through in-stream processing for large distances below plants and some showing high rates of processing and retention. This study focuses on Sandy Run, a small, suburban stream in Montgomery County, PA, that receives effluent from two plants, where effluent makes up an estimated 50% of outlet discharge at baseflow. Two sites were monitored in late summer baseflow using high-temporal loggers to evaluate nitrate and phosphate retention with distance below the plants. Effluent quantity was monitored immediately below the effluent outfalls using specific conductivity as a conservative signal of solute fluctuations throughout the day. A site one km downstream showed diel nitrate changes, but, despite moderate gross primary productivity (GPP) and ecosystem respiration (ER) rates, there was little net retention of nutrients and the diel nitrate signal can be attributed to advection and dispersion of variable upstream effluent. A site 5.4 km below the plant showed a diel nitrate signal as well, but baseflow daily hysteresis plots of nitrate and specific conductivity showed the effluent and nitrate peaks did not coincide. Instead, the effluent input signal was seen overnight, but there was in-stream removal and release processes during the day. Over the distance to this site, the stream was metabolizing some of the high nutrient loads, although GPP and ER rates were lower. It is important to understand sub-daily changes in nutrient processing to fully quantify the impacts of effluent on small streams at different scales. Furthermore, looking at the diel signal without considering conservative transport would over-estimate in-stream processing.

Keywords: nitrogen cycling; wastewater treatment plant; urban stream; high-temporal sensor; in-stream metabolism; gross primary productivity (GPP); ecosystem respiration (ER); daily hysteresis

1. Introduction

Understanding nutrient cycling is important for improving stream health in nutrient-enriched systems and predicting loads to receiving waters. Major pathways for dissolved inorganic nitrogen (DIN) transformations include assimilation of DIN into biomass, nitrification of NH_4^+ to NO_3^- , and denitrification of NO_3^- to gaseous products, including N_2 gas when denitrification goes to completion (Ribot et al., 2012). The multiple sources and pathways for DIN make it difficult to characterize ecosystem response when measuring a single species of DIN, and there is a need for geochemical tools to improve monitoring and prediction of stream metabolism. The sources of soluble reactive phosphorous (SRP) in streams are predominantly wastewater and overland runoff from sources such as fertilizer and organic matter (Jarvie, Neal, & Withers, 2006). However, the majority of overland runoff is particulate, typically >50% and up to 90% (Withers & Jarvie, 2008). Thus, SRP transformation in streams often involves moving from the dissolved to the particulate phase (sediment-bound P); the importance of sediment-bound P contrasts with N, along with the lack of atmospheric exchange. Both biological uptake and abiotic sorption of SRP occur during baseflow, leading to retention in rivers (Withers & Jarvie, 2008) with rapid SRP uptake in forested streams (Mulholland, Marzolf, Webster, Hart & Hendricks, 1997). Lower uptakes rates were observed in an urban stream by Ryan, Packman, and Kilham (2007) and were dominated by abiotic processes suggesting retention in sediments is dominant (Haggard, Stanley, & Storm, 2005). Furthermore, bioavailability of sediment-bound P is likely limited and release of accumulated P in sediment could take decades or centuries (Goyette, Bennett,

& Maranger, 2018). Point sources of nutrients to streams increase biotic stress (Gücker, Brauns, & Pusch, 2006), increasing the importance of understanding how nutrients are being retained and exported.

1.1 Wastewater treatment plants as nutrient sources

Wastewater treatment plants (WWTPs) increase nutrient loading to streams. While primary treatment aims to remove organic material from sewage, secondary and tertiary treatment processes decrease DOC, DIN, and phosphorus concentrations in effluent (Carey & Migliaccio, 2009; Worrall, Howden, Burt, & Bartlett, 2019). Secondary processes are now ubiquitous in WWTP technology across the U.S. as plants meet their National Pollution Discharge Elimination System (NPDES) permits, regulated through the U.S. Environmental Protection Agency (Carey & Migliaccio, 2009). High nutrient loads to streams below WWTP effluent outfalls lead to eutrophication issues, both locally and downstream (Figuerola-Nieves, McDowell, Potter, & Martínez, 2016; Goyette et al., 2018; Haggard et al., 2005; Martí, Aumatell, Gode, Poch, & Sabater, 2004) along with changes to biological communities (Gücker et al., 2006; Price, Ledford, Ryan, Toran, & Sales, 2018; Ribot et al., 2012). A range of impacts of large nutrient loads below WWTP effluent outfalls to nutrient cycling have been observed, requiring more research.

Increased nutrient loads from WWTP effluent do not have a uniform, predictable response downstream. Many studies have found a decrease in net nutrient retention below plants and increased nutrient export in both small and large rivers (Figuerola-Nieves et al., 2016; Haggard, Storm, & Stanley, 2001; Martí et al., 2004). Uptake lengths for NH_4^+ usually decrease due to nitrification of NH_4^+ discharged in effluent, but uptake lengths increase for NO_3^- and SRP increase in length and, in some cases, uptake does not occur due to over-fertilization (Gammons, Babcock, Parker, & Poulson, 2011; Haggard et al., 2005; Martí et al.,

2004; Merseburger, Martí, & Sabater, 2005). Other signs of minimal in-stream processing of nitrogen include the downstream propagation of a typical two-peak diel signal from a WWTP up to 16 km below the plant (Halliday et al., 2014). Stream size plays a role in net retention, with large rivers such as the Chattahoochee River and Middle Rio Grande showing diminished uptake capacity compared to small streams, sometimes requiring 180 km of river length to return to pre-WWTP concentrations (Gibson & Meyer, 2007; Oelsner, Brooks, & Hogan, 2007). In contrast, some studies have also seen a decrease in nitrate uptake length below WWTP outfalls, indicative of increased retention, attributing it to in-stream denitrification hotspots spurred by discharge of DOC from WWTPs, although there is the potential this varies seasonally (Gücker et al., 2006; Rahm, Hill, Shaw, & Riha, 2016; Ribot et al., 2012). Uptake length, however, does not account for variations in discharge or concentration, while calculations of uptake velocity (also called the mass transfer coefficient) and net nutrient uptake rate consider changes in velocity, depth and concentration. Uptake rates have been shown to increase below WWTPs while uptake velocity decreases in some studies (Figuroa-Nieves et al., 2016; Haggard et al., 2005); other studies show increases in both uptake rate and uptake velocity (Gücker et al., 2006). Along with a non-uniform response in nutrient retention efficiency below WWTPs, these measures all integrate uptake and release processes below the effluent signal, still leaving questions about competition between rates of removal and release.

1.2 High-temporal sensors and the impact on understanding nutrient processing

The fine temporal scale observations of in-stream concentrations provided by high-temporal nutrient loggers have transformed our understanding of in-stream processes, especially for nitrogen (Burns et al., 2019). The high frequency sampling provided by data loggers has shown that diel patterns in nitrate signals can be out of phase with the timing of

metabolic signals indicated by dissolved oxygen diel cycles (Hensley & Cohen, 2016; Nimick, Gammons, & Parker, 2011). Heffernan and Cohen (2010) used high-temporal sensors to identify the relationship between denitrification and the previous day's photosynthesis; a negative relationship between gross primary productivity (GPP) and nocturnal nitrate was indicative of denitrification depending on autochthonous carbon production. Pellerin et al. (2009) noted the impact of hydrologic transport on diel nitrate signals and Hensley and Cohen (2016) showed with models that a lack of a diel signal does not indicate a lack of in-stream nitrogen processing. Instead, concentration patterns, such as diel nitrate signals, are an integration of dispersion, storage, and local processing in systems with constant nitrate inputs. Hydrologic factors such as evapotranspiration can also lead to seasonal shifts in nutrient cycles (Auber & Breuer, 2016). High-temporal phosphorus data is rarer, with studies focusing on agricultural catchments (Jordan, Arnscheidt, McGrogan, & McCormick, 2005) or over single-day time frames (Scholefield et al., 2005). However, automatic grab samples for phosphate analysis have failed to show diurnal signals in concentration that are captured by *in situ* loggers (Bieroza & Heathwaite, 2015). In addition, while temporal variability is important to monitor and understand, understanding spatial dynamics is also vital to fully capturing a system (Crawford et al., 2015). Most of these studies using high-temporal sensors have focused on forested systems rather than streams impacted by humans.

Nutrient sensors have the potential to unravel some of the complexities of signals in urban streams and other disturbed systems (Burns et al., 2019; Pellerin et al., 2016). High temporal data has allowed for detailed storm analysis of nutrient dynamics, with concentration-discharge relationships being used to evaluate sources of nutrients to streams (Burns et al., 2019). Bowes et al. (2015) used distinct patterns in hysteresis plots of nutrients and flow to characterize different sources of nutrients including remobilized bed sediments,

WWTPs, and diffuse inputs. Koenig, Shattuck, Snyder, Potter, and McDowell (2017) used nitrate-discharge and DOC-discharge relationships to evaluate the decoupling of nitrate and carbon in developed watersheds in New Hampshire. Duncan, Welty, Kemper, Groffman, and Band (2017) used multi-year records of nitrate in Baltimore, MD to show chemostatic nitrate response to storms through time. Sensors are also able to piece apart flux data, with long term monitoring datasets showing that systems with anthropogenic inputs can have higher loads in the summer, when stream metabolism would otherwise be expected to reduce loads (Halliday et al., 2014). High-temporal sensors have helped identify source and transport limitations to nutrients in highly modified landscapes.

Questions still remain about the relationship between nutrients and in-stream processing in anthropogenic systems. High-temporal sensors have been used to evaluate nitrate patterns in agricultural streams, with low concentrations observed in the afternoon and high concentrations in the early morning due to higher assimilation during photosynthesis than denitrification at night (Jones et al., 2018). High frequency logging has shown that variations in anthropogenic inputs can overprint diel nitrate patterns, which can make predictions of load from grab samples uncertain (Carey, Wollheim, Mulukutla, & Mineau, 2014; Duan, Powell, & Bianchi, 2014; Pellerin et al., 2009). High frequency nutrient sensors have shown a dual peak in discharge and nutrients related to WWTP output when flows are low and the WWTP discharge is a greater percentage of flow (Halliday et al., 2015; Wade et al., 2012). Human creation of waste varies in rate through the day, with high levels of waste in the morning when people wake up and a second peak in the evening when people return home; levels of waste creation are low overnight. This signal is then passed to the effluent after treatment resulting in two peaks in effluent quantity each day driven by changes in the quantity of waste reaching the plant. The combination of multiple sources and sinks in

human-impacted streams makes fine-scale sampling provided by sensors vital to understanding processing.

This paper looks at the relationship between in-stream metabolism and diel nutrient signals to quantify in-stream processing and to evaluate how nutrient retention efficiency changes with distance from a WWTP. A better understanding of how the high nutrient loads from WWTPs evolve with distance from the plant is needed as management efforts continue to address local and downstream eutrophication issues. Unlike previous work that uses temporal sensors in natural streams where input signals are often assumed to be constant, the WWTP effluent signal is known to change throughout the day (Halliday et al., 2015; Wade et al., 2012). This shifting input confounds attempts to piece apart uptake and removal processes in WWTP-impacted streams using traditional methods.

A second objective of this paper is to evaluate single-station changes in diel nitrate concentration compared to a conservative transport signal, in this case specific conductivity, for calculating sub-daily shifts in dominant nitrogen pathways below WWTPs using baseflow hysteresis plots. While the two-station method for nitrate is ideal to parse out changes in signal due to transport versus processing (Hensley & Cohen, 2016), the high expense of in-situ sensors still prohibits it for most monitoring programs. The single-station technique builds off the idea of using a conservative tracer to normalize longitudinal changes in nitrate to calculate uptake length but instead approaches the problem from a temporal standpoint. (Haggard et al., 2001; Martí et al., 2004; Stream Solute Workshop, 1990). This distinction is important because without piecing apart the relative importance of evolving input signal, advection, dispersion, and processing, diel signals could be used to attribute all changes to in-stream processing.

2. Methods

2.1 Field Sites

Wissahickon Creek is a third-order stream located in Montgomery and Philadelphia Counties, Pennsylvania, USA, that flows into the Schuylkill River. The main stem is 43.5 km long, with a total drainage length of 184.6 km, covering a watershed of 164.9 km² (PWD, 2007). Overall, 27% of the watershed land cover in Montgomery County is impervious surface and another 24% is semi-pervious (such as lawns). The largest tributary is the second-order Sandy Run, which had a total length of 26.7 km (including its tributaries) (PWD, 2007). The stream is listed as impaired due to nutrients and siltation (EPA, 2003).

Two WWTPs discharge into Sandy Run and its tributary (Figure 1). Abington WWTP is permitted to discharge 17.7 million L day⁻¹ to Sandy Run, but averages 11 million L day⁻¹ or about 90% of baseflow at the discharge location. This plant uses activated sludge with alum and polyaluminum chloride used to remove phosphorus and aeration chambers to convert ammonia to nitrate. Abington effluent averages 0.2 mg N/L of ammonia. The second plant, Upper Dublin WWTP, is on a small tributary further downstream, Pine Run, and is permitted to discharge 5 million L day⁻¹ although it averages closer to 3 million L day⁻¹. Upper Dublin WWTP has a trickling filter and activated sludge that removes phosphorus with ferric chloride with polymer. Upper Dublin effluent typically has high ammonia concentrations of 1-2 mg N/L. Neither plant has tertiary treatment. After the confluence with Sandy Run, the combined input from the two WWTPs is about 50% of baseflow with only 10% of that coming from Upper Dublin. Depth and specific conductivity were monitored in-stream immediately below the two WWTPs at 15-minute intervals from May 11, 2017 to March 19, 2018.

Sandy Run was monitored at two sites downstream of these WWTP discharges for roughly week-long periods. The site identified as the “downstream site” was 5.4 km below the Abington WWTP and below the confluence with Pine Run and Upper Dublin WWTP; the

downstream site was monitored from 23:00 EST on September 3, 2016 to 18:00 EST on September 8, 2016. Baseflow discharge during this period was around 250 L/s. The second site, 1.0 km below the Abington WWTP (from here on identified as the “near site”), was monitored from 10:00 EST on August 11, 2017 until 23:00 on August 17, 2017, and is above the confluence with the tributary containing Upper Dublin WWTP discharge.

2.2 Instrumentation

In-stream monitoring was conducted using high-temporal sensors. Depth, specific conductivity, dissolved oxygen, and nitrate were all measured at hourly intervals at both the downstream and near sites. Depth was measured with an Onset HOBO water level logger with a barometric logger located within 3 km for correction, while specific conductivity and dissolved oxygen were measured with a YSI EXO2 multiprobe, with all probes calibrated before deployment. Nitrate was measured with a Satlantic SUNA V2 optical nitrate sensor that was calibrated in the lab before deployment. Each nitrate measurement collected four concentration values, of which the average is reported. The average standard deviation among the four samples was 0.02 mg N/L. Phosphate was measured at the downstream site using Sea-Bird Coastal HydroCycle-PO₄ phosphate analyzer. It collected hourly samples, running a calibration standard every six samples. Sample error is reported by Sea-Bird Coastal as 0.01 mg P/L. Equipment malfunction did not allow for high-frequency phosphate monitoring at the near site in 2017. Grab samples were collected to confirm logger performance and analyzed in the lab using a Dionex ICS-1000 for nitrate and a Thermo Scientific iCAP 7000 ICP-OES for total dissolved phosphorous. Grab samples confirmed the trends in concentration measured by the loggers. Depth and specific conductivity were measured immediately below each WWTP outflow using Onset HOBO depth and specific conductivity loggers.

2.3 GPP, ER, Assimilation, and FFT

Dissolved oxygen diel cycles were used to estimate stream metabolism using StreamMetabolizer (Appling, Hall, Yackulic, & Arroita, 2018). The reaeration coefficient (k) was calculated at night when autotrophic metabolism was absent from the signal, and k was pooled among days with a normal distribution. Ten days were used to model GPP/ER at the downstream site and eight days were used at the near site, using periods when the signal was not interrupted by storms or other interference to the logger. Autotrophic assimilation of N was also estimated using GPP derived from diel O₂ signals (Hall & Tank, 2003), assuming net heterotrophic production as 50% of GPP and a net photosynthetic quotient of 1 (Heffernan & Cohen, 2010; Rode, Halbedel, Anis, Borchardt, & Weitere, 2016). Fast Fourier transformations (FFT) were calculated in Matlab on the entire temporal series of depth, specific conductivity, nitrate, and phosphate to identify frequencies in the time-series with the highest powers and to help deconvolute transport signals from in-stream processing signals.

2.4 Hysteresis

Shifts in WWTP quantity, and thus flux of solutes, will result in downstream shifts in water quality throughout the day, combined with shifts in concentration due to advection and dispersion of all solutes and retention (assimilation and denitrification) or addition (mineralization and nitrification) for nutrients, nitrogen specifically. In order to account for advection and dispersion, specific conductivity is assumed to be a conservative signal that incorporates both changing source flux of effluent throughout the day and advection and dispersion during downstream travel (Martí et al., 2004). The Upper Dublin WWTP is assumed to have minimal impact on changes in in-stream concentrations or discharge due to the fact that depth and specific conductivity measured immediately below the outfall show

minimal daily fluctuations (only 0.01 m depth in contrast to 0.05 m at Abington, and no diurnal pattern in August) during the period of baseflow monitoring of the nutrients (Fig. S1) and overall discharge of Pine Run is small compared to discharge in Sandy Run (around 10% during the study period). In contrast, the stream immediately below the Abington WWTP outfall shows that specific conductivity and water depth both increase starting around 5:00 each morning. Both stay high through the day, decreasing around midnight (Fig. S2). There is a slight decoupling of specific conductivity and depth in the evening, with specific conductivity beginning to decrease before depth. We attribute this observation to incomplete mixing between the channel and pool where loggers were placed below the WWTP, but specific conductivity is still the best conservative tracer to account for transport at each site. Therefore, concentration changes downstream of the WWTP can be differentiated between changes due to changing WWTP effluent and changes due to metabolic processing by comparing specific conductivity to bioavailable constituents. Groundwater inflow is assumed to be minimal at both sites as discharge does not change much with distance.

3. Results

3.1 Near Site

At the near site, the stream was at baseflow during monitoring except for a small storm of approximately 3 mm of rain on August 15th, which caused a small increase in stream depth and a small dilution in all dissolved ion concentrations that were being measured. At baseflow, depth varied from 0.07 to 0.15 m (Fig. 2a), showing the typical two-peak WWTP signal (Halliday et al., 2014; Wade et al., 2012) with early morning troughs observed from 5:00-7:00 and high power frequencies at 0.5 and one days (Table 1, Fig. S3). Excluding the storm, specific conductivity ranged from 715 to 798 $\mu\text{S}/\text{cm}$, with daily minimum at 10:00-11:00, offset from the water level signal due to advection and dispersion of the effluent plume

(Fig. 2a). Nitrate ranged from 6.7 to 14.4 mg N/L and the storm causes a slight dilution of nitrate, but not beyond the typical diel minimum concentration (Fig. 2b). Nitrogen troughs are typically timed with specific conductivity minima each day, between 10:00 and 11:00. FFT results show high power at one day for both specific conductivity and nitrate, emphasizing the strong diel signal in both solutes (Table 1, Fig. S3). Dissolved oxygen had a typical diel signal, ranging from 6 to 11.1 mg/L, slightly suppressed the day of the rain event (Fig. 2c). A local watershed organization sampled for ammonia near the loggers one day during our week of monitoring and concentration was less than 0.2 mg N/L (WVWA, 2017). Hysteresis patterns between depth and specific conductivity at this site show a counter-clockwise pattern (Fig. S4), while the pattern between specific conductivity and nitrate is linear (Fig. 3), except on August 15th to 16th, when there was a small storm and a counterclockwise conductivity and nitrate pattern on August 14th.

3.2 Downstream Site

At the downstream site, discharge was at baseflow the entire period, with the most recent precipitation being 2 mm of rain on September 1st, two days prior to the monitoring period. Depth at the site ranged from 0.07 to 0.12 m, with a strong daily two-peak signal (Fig. 2d) and with high power at 0.5 and one days frequencies (Table 1, Fig. S5). These two peaks are created by downstream propagation of discharge variations from Abington WWTP, with the impact of the confluence of Pine Run insufficient to create a high-power frequency. This results in nightly low discharge flows coming through between 8:00 and 12:00. Specific conductivity ranged from 781 to 870 $\mu\text{S}/\text{cm}$, with a consistently upward drift over the observation period, potentially due to decreasing baseflow discharge (Fig. 2d). Overall, the specific conductivity had a small diel signal, with trough timing varying, but peak specific conductivity was consistently seen from 14:00-15:00 and this diel signal shows up as high

power at one day (Table 1, Fig S5). Patterns in specific conductivity are also potentially influenced by mixing with Pine Run above this site, however, the Upper Dublin WWTP has limited impact on depth or specific conductivity below its outfall (Fig. S1) and Pine Run is estimated to only be 10% of the flow at this site, minimizing its importance. Therefore, we believe a majority of the in-stream solute signal at the downstream site can be attributed to hydrologic transit and in-stream processing happening in Sandy Run. Nitrate ranges from 6.3 to 11.4 mg N/L, with a daily peak just before sunrise (3:00-7:00) for 4 of the 5 days and a trough in the early afternoon (13:00-15:00) (Fig. 2e). Nitrate has a strong frequency at one day at this site, with minimal power at 0.5 days (Table 1, Fig. S5). Ortho-phosphate ranges from 0.51 to 0.97 mg P/L (Fig. 2f). P exhibits a diurnal WWTP signal, with one minimum around 14:00-15:00. Phosphate has important frequencies at 0.5 and one days, similar to depth and specific conductivity (Table 1, Fig. S5). However, it does not have a daily peak, instead has plateau concentration from the evening to mid-day the next day. Dissolved oxygen has a slightly smaller diel signal, showing a broad trough, and ranging from 5.6 to 9.4 mg/L (Fig. 2g). Samples collected by a local watershed organization indicate ammonia concentrations are typically below 0.2 mg N/L at this site in early September (WVWA, 2017). Depth and specific conductivity show a clockwise hysteresis at this site (Fig S6). Specific conductivity and nitrate also have a clockwise hysteresis pattern, although sub-daily counter-clockwise loops form in the early morning and late evening on September 5th and 6th, 2016 (Fig 4). In addition, specific conductivity and orthophosphate have a negative linear relationship (Fig. 5).

3.3 GPP, ER, and Assimilation

GPP for the near site averaged $3.9 \text{ g O}_2 \text{ m}^{-2} \text{ d}^{-1}$ and dropped to $0.2 \text{ g O}_2 \text{ m}^{-2} \text{ d}^{-1}$ at the downstream site (Table 2). Similarly, ER was higher at the near site, averaging $-6.3 \text{ g O}_2 \text{ m}^{-2}$

d^{-1} and dropping to $-0.7 \text{ g O}_2 \text{ m}^{-2} \text{ d}^{-1}$ at the downstream site. Both sites were net heterotrophic during all days, with net ecosystem productivity (NEP) averaging $-2.3 \text{ g O}_2 \text{ m}^{-2} \text{ d}^{-1}$ at the near site and $-0.4 \text{ g O}_2 \text{ m}^{-2} \text{ d}^{-1}$ at the downstream site. Near the WWTP, the model fit the observed DO signal well (Fig S7). The model did not fit peak DO as well at the downstream site potentially driven by noise in the nightly DO signal, so GPP may be underestimated. Despite this, the model fit well on September 6th resulting in a GPP of $0.3 \text{ g O}_2 \text{ m}^{-2} \text{ d}^{-1}$ and ER of $-0.7 \text{ g O}_2 \text{ m}^{-2} \text{ d}^{-1}$, very similar to the overall average (Fig. S7).

Using GPPs calculated during the periods of observation (Table 2) to estimate autotrophic assimilation (Hall & Tank, 2003; Rode et al., 2016), we can see that a minimum of $0.05 \text{ g N m}^{-2} \text{ d}^{-1}$ and a maximum of $0.15 \text{ g N m}^{-2} \text{ d}^{-1}$ would be assimilated near the WWTP (when C/N ratio is 8.5, as reported in Rode et al., 2016). Further downstream, where productivity is even lower, GPP could only account for at most $0.008 \text{ g N m}^{-2} \text{ d}^{-1}$ (with a minimum of $0.003 \text{ g N m}^{-2} \text{ d}^{-1}$). While actual C/N ratios of the algal biomass are unknown at our site, the mass of assimilated nitrogen will only continue to decrease as the C/N ratio increases, so these rates would be upper limits of the autotrophic assimilation capacity of the stream based on measured productivity. This disconnect between the diel N signal and actual potential productivity is why it is so important to consider hydrologic transit of the shifting input source.

4. Discussion

4.1 WWTP Signal Transit

Comparison of depth and specific conductivity signals show how the WWTP discharge signal is transported downstream. Immediately below the Abington WWTP, depth and specific conductivity signals are roughly synchronized, increasing between 5:00 and 6:00 and decreasing after midnight (Fig S2). This pattern is supported by frequency powers

immediately below the plant, with both signals having the strongest power at one day, and the second strongest frequency in depth is at 0.5 days, driven by the twice-daily changes in effluent discharge (Fig S8). The 0.5 days frequency is not as strong in the specific conductivity time-series, which we attribute to incomplete mixing at our logger location below the effluent outfall (Fig. S8). At the near site, there is a clear counter-clockwise daily hysteresis pattern between depth and specific conductivity (Fig. S4). This hysteresis is driven by the depth signal being transported by pressure wave celerity while solute advection and transport, which is slower, controls the specific conductivity signal (Fig 2a; McDonnell & Beven, 2014). This is confirmed as both signals at this site have strong frequency at one day (Table 1, Fig S3) but only depth matches the frequencies immediately below the WWTP with a strong frequency at 0.5 days (Fig S8). Because the specific conductivity signal is the solute signal and incorporates advection and dispersion, it is used to account for changes in WWTP solutes to differentiate source changes from nutrient processing.

At the near site, there is a generally linear relationship between specific conductivity and nitrate, except during disruption by the small storm on August 15th (Fig. 3). On August 14th and 16th, there was a short period in the afternoon where nitrate and specific conductivity become uncoupled, with specific conductivity decreasing while nitrate increases by a small amount. The decrease in specific conductivity is a sign that a low effluent signal has reached the site, and nitrate is expected to decrease as well. However, since nitrate is increasing, this period signifies release of nitrate from an in-stream process, most likely mineralization of biomass (Gücker et al., 2006; Martí et al., 2004). The periods of linear relationship (Fig. 3) indicate the diel signal in nitrate is driven by advection and dispersion of the variable WWTP effluent source plume and not in-stream processing, as both specific conductivity and nitrate are changing together (Fig. 6). This transport signal is also supported by FFT results, which show depth, specific conductivity and nitrate all have powerful frequencies at one day (Table

1, Fig S3). Depth shows the twice-a-day peak, with a strong frequency at 0.5 days, but neither specific conductivity nor nitrate show that frequency. Instead, they both have high power at two days (Table 1). GPP and ER rates indicate $0.15 \text{ g N m}^{-2} \text{ d}^{-1}$ are being assimilated by autotrophs at this site, but the lack of impact on nitrate concentrations shows net retention is minimal, overwhelmed by the high nutrient inputs to the stream from the effluent as has been seen in other WWTP studies (Figuroa-Nieves et al., 2016; Haggard et al., 2001; Martí et al., 2004). Without considering the downstream advection and dispersion of the changing effluent, incorrect conclusions could easily be drawn from the nitrate signal at this site, and the strong diel signal (Fig. 2b) could be interpreted as a major location of processing. The lack of net retention at this site is supported by multiple studies showing in-stream nutrient retention decreased below WWTPs, resulting in net nitrogen export increasing.

As the signal continues to be transported to the downstream site, specific conductivity and depth still have strong frequencies at 0.5 and one day, indicating the conservative transport of water and solutes is still driven by changes in WWTP effluent (Table 1, Fig S5). While this site is downstream of the Upper Dublin WWTP, discharge and load calculations indicate it only constitutes 10% of the signal. In addition, the WWTP signal is not apparent immediately below the plant (Fig. S1) and FFT frequencies are not related to typical WWTP timings. Because of this, we assume the dominant WWTP signal at the downstream site is from the Abington plant. Different physical processes continue to control these signals, with depth changing from upstream pressure head celerity and specific conductivity changing due to flow velocity (McDonnell & Beven, 2014), resulting in hysteresis behavior (Fig. S6). In contrast to specific conductivity, nitrate does not have a strong frequency at 0.5 days, but does have a high power at one day, indicating that in-stream processing is changing the nitrate signal (Table 1). In addition, the relationship between specific conductivity and

nitrate at the downstream site is no longer linear (Fig. 4). Periods where nitrate and specific conductivity increase together are still interpreted as periods of time where the dominant signal is WWTP transport. There are, however, times when the signals do not move together, and these indicate periods of removal, when specific conductivity increases while nitrate decreases, or release, when specific conductivity decreases while nitrate increases (Fig. 6). Each of the observed days shows roughly the same pattern: the WWTP signal comes through at night, until about 3:00, with both nitrate and specific conductivity increasing (Fig. 4 and 6). The signal then shifts to a removal signal until 13:00-15:00, during which specific conductivity increases but nitrate concentrations decrease. The removal signal is a sign of processes such as assimilation or denitrification, but consistent timing of this process dominating during the day, usually ending in the early afternoon, gives weight to the hypothesis that it is an photosynthesis-driven assimilative signal. After this, the nitrate signal shifts to a release pattern, with specific conductivity decreasing but nitrate increasing from 15:00 until 20:00. Increases in nitrate have been seen below WWTPs in other locations, and they have been attributed to subsurface inputs and in-stream release processes (Figueroa-Nieves et al., 2016; Martí et al., 2004; Merseburger et al., 2005; Ribot et al., 2012). We do not have any indications of large groundwater nitrate inputs in this system, and low ammonium concentrations eliminate nitrification of WWTP effluent as a possibility, so this release is most likely due to mineralization of organic matter that has been produced in-stream below the plant (Figueroa-Nieves et al., 2016; Martí et al., 2004). Finally, the signal returns back to a WWTP signal overnight, from 20:00 to midnight, with both specific conductivity and nitrate concentrations increasing. The persistence of this pattern over this baseflow monitoring period shows that in-stream processes occurring over the 5.4 km of distance below the plant are changing daytime nitrate concentrations while at night WWTP effluent signals dominate.

In addition to these relationships with nitrate, there is a negative linear relationship between specific conductivity and P at the downstream site (Fig. 5), with lowest phosphate concentrations in the early afternoon. High phosphorus concentrations are sourced from the WWTP, but the afternoon decreases in phosphate could be driven by uptake and not by a changing source. The phosphate time-series has high power at 0.5 and one day frequencies (Table 1, Fig. S5), potentially an underlying WWTP effluent signal. However, the correlated timing between minimum phosphorus concentrations and peak dissolved oxygen concentrations gives weight to a hypothesis of photosynthetic controls on nutrient uptake in the afternoon at this site (Fig. 2f and 2g; Cohen et al., 2013). With low GPP rates at this site (Table 2), local processing alone may not be enough to cause the daily 0.2 mg P/L changes in concentration and so inorganic transformation of P (i.e., sorption) may also be driving these concentration changes. However, decoupling these two drivers is not possible with the data collected (as noted in Cohen et al., 2013; Withers & Jarvie, 2008).

Other studies have used stormwater hysteresis plots to identify different behavior of N and P retention in streams (Aguilera & Melack, 2018), antecedent moisture controls (Bowes et al., 2015; Baker & Showers, 2019), and source term limitations (Bowes, House, Hodgkinson, & Leach, 2005; Bieroza & Heathwaite, 2015). This study differs by using baseflow hysteresis to contrast conservative behavior and processing. The variations observed help distinguish WWTP signals and better quantify changes in processing with distance downstream of the WWTP.

4.2 Impact of shifting input signal on N removal

GPP and ER rates are higher closer to the WWTP compared to further downstream, but even near the plant they are not particularly high. Near the plant, GPP ranges from 2.1 to 5.9 g O₂ m⁻² d⁻¹, falling to 0.1 to 0.3 g O₂ m⁻² d⁻¹ at the downstream site (Table 2), both low

Accepted Article

rates compared to GPP rates of 3 to 47 g O₂ m⁻² d⁻¹ measured in other high-nutrient streams during the summer (Alberts, Beaulieu, & Buffam, 2017; Gücker et al., 2006). Our stream is net heterotrophic at both sites, with ER ranging from -4.1 to -7.7 g O₂ m⁻² d⁻¹ near the plant and -0.5 to -0.8 g O₂ m⁻² d⁻¹ downstream. Gücker et al. (2006) is one of the only studies that has reported GPP below WWTPs. Their Erpe River site is the most similar to ours, with downstream discharge of approximately 500 L/s and nitrate concentrations of 6.5 mg N/L, although their phosphate concentrations were much lower. At this site, GPP below the WWTP ranged from 47 g O₂ m⁻² d⁻¹ in the summer to <0.1 g O₂ m⁻² d⁻¹ during the winter. In addition, ER was 59 g O₂ m⁻² d⁻¹ in the summer and the site was always net heterotrophic. No data are reported about light conditions at their site, but our stream is highly shaded in the summer, potentially driving our low GPP rates compared to theirs. Alberts et al. (2017) reported GPP rates of 2 to 9 g O₂ m⁻² d⁻¹ and ER rates of -4 to -9 g O₂ m⁻² d⁻¹ in an urban shaded reach during summer, but nitrate concentrations were much lower (0.03 mg N/L) and discharge was not reported. Other studies that reported higher GPP and ER than we measured had streams with no riparian cover (Clapcott, Young, Neale, Doehring, & Barmuta, 2016) or had much lower discharge (Beaulieu, Arango, Balz, & Shuster, 2013). Our rates of GPP and ER at the near site are similar to those seen in Alberts et al. (2017) but our nutrient concentrations are much higher, and our rates are lower than those seen in a similar WWTP-impacted stream. GPP and ER rates at our downstream site are lower than any reported under similar conditions.

N uptake calculated from GPP rates are much lower than those that would be estimated from the diel nitrate signal using a method like that in Heffernan & Cohen (2010). The incompatibility is due to the diel signal also including the shifting source signal, a fact that could easily be overlooked especially if grab samples are collected for water quality monitoring. GPP and ER rates indicate metabolic activity at the site near the WWTP, while

the nitrate concentration closely tracks the specific conductivity signal. This tracking shows the lack of net nitrogen retention in streams below WWTPs due to extremely high nitrate loads (Martí et al., 2004). Further from the plant, GPP and ER decrease by an order of magnitude. The shift in the timing of the nitrate and specific conductivity signals at the site downstream are interpreted to be signs of processing over the reach between the sites, both removal (assimilation or denitrification) or release (mineralization or nitrification). Because we do not have calculations of GPP at the sub-daily scale, we cannot calculate rates of N assimilation that would be required during periods of removal. Concentrations fall by about 1.5 to 3 mg N/L during these periods, however, indicating there is substantial in-stream processing.

5. Conclusions

High-frequency sensor data below WWTP outfalls on small streams illuminates detailed information about in-stream processing. While the two-station method is the best to calculate in-stream processing in these situations, the cost of nutrient loggers is still high. Instead, this paper highlights the information about in-stream processing that can be inferred by comparing conservative and non-conservative solute signals from a single station. Nitrate had a diel pattern at our site located near the WWTP, which could be mis-interpreted as processing if the variable WWTP effluent impact is not considered. However, when variable WWTP input variation is accounted for, our site located near the WWTP did not have any indications of net nutrient retention despite GPP and ER rates similar to other studies below WWTPs. Further downstream, daily baseflow hysteresis patterns show periods when nitrate and specific conductivity become out of synchronization, indicating nitrate retention and release. The timing of these shifts during daylight indicate they are potentially driven by assimilation, with mineralization of in-stream biomass in the evenings. Using the single-

station method, we have shown that a small stream that is 50% effluent at baseflow has some nutrient retention within 5 km of the outfall, but that temporal nutrient patterns alone cannot be assumed to be metabolically driven; instead assessment must account for variable sources and transport.

References

Aguilera, R., & Melack, J. M. 2018. Concentration-discharge responses to storm events in coastal California watersheds. *Water Resources Research* 54(1):407-424.

Alberts, J. M., Beaulieu, J. J., & I. Buffam. 2017. Watershed land use and seasonal variation constrain the influence of riparian canopy cover on stream ecosystem metabolism. *Ecosystems* 20:553-567.

Appling, A. P., Hall Jr, R. O., Yackulic, C. B., & M. Arroita. 2018. Overcoming equifinality: leveraging long time series for stream metabolism estimation. *Journal of Geophysical Research-Biogeosciences* 123:624-645.

Aubert, A. H. & L. Breuer. 2016. New seasonal shift in in-stream diurnal nitrate cycles identified by mining high-frequency data. *PLoS ONE* 11(4).
doi:10.1371/journal.pone.0153138.

Baker, E. B., & Showers, W. J. 2019. Hysteresis analysis of nitrate dynamics in the Neuse River, NC. *Science of the Total Environment* 652:889-899.

Beaulieu, J. J., Arango, C. P., Balz, D. A., & W. D. Shuster. 2013. Continuous monitoring reveals multiple controls on ecosystem metabolism in a suburban stream. *Freshwater Biology* 58:918-937.

Bieroza, M. Z. & A. L. Heathwaite. 2015. Unravelling organic matter and nutrient biogeochemistry in groundwater-fed rivers under baseflow conditions: uncertainty in in situ high-frequency analysis. *Science of the Total Environment* 572: 1520-1533.

Bowes, M. J., House, W. A., Hodgkinson, R.A., & Leach, D. V. 2005. Phosphorus-discharge hysteresis during storm events along a river catchment: the river Swale, UK. *Water Resources* 39(5):751-762.

Bowes, M. J., Jarvie, H. P., Halliday, S. J., Skeffington, R. A., Wade, A. J., Loewenthal, M., ... & E. J. Palmer-Felgate. 2015. Characterizing phosphorus and nitrate inputs to a rural river using high-frequency concentration-flow relationships. *Science of the Total Environment* 511:608-620.

Burns, D. A., Pellerin, B. A., Miller, M. P., Capel, P. D., Tesoriero, A. J., & J. M. Duncan. 2019. Monitoring the riverine pulse: applying high-frequency nitrate data to advance integrative understanding of biogeochemical and hydrological processes. *WIREs Water*. doi:10.1002/wat2.1348.

Carey, R. O. & K. W. Migliaccio. 2009. Contribution of wastewater treatment plant effluents to nutrient dynamics in aquatic systems: a review. *Environmental Management* 44: 205-217.

Carey, R. O., Wollheim, W. M., Mulukutla, G. K., & M. M. Mineau. 2014. Characterizing storm-event nitrate fluxes in a fifth order suburbanizing watershed using in situ sensors.

Environmental Science & Technology 48:7756-7765.

Clapcott, J. E., Young, R. G., Neale, M. W., Doehring, K., & L. A. Barmuta. 2016. Land use affects temporal variation in stream metabolism. *Freshwater Science* 35(4):1164-1175.

Cohen, M. J., Kurz, M. J., Heffernan, J. B., Martin, J. B., Douglass, R. L., Foster, C. R., & R. G. Thomas. 2013. Diel phosphorus variation and the stoichiometry of ecosystem metabolism in a large spring-fed river. *Ecological Monographs* 83(2):155-176.

Crawford, J. T., Loken, L. C., Casson, N. J., Smith, C., Stone, A. G., & L. A. Winslow. 2015. High-speed limnology: using advanced sensors to investigate spatial variability in biogeochemistry and hydrology. *Environmental Science & Technology* 49:442-450.

Duan, S., Powell, R. T., & T. S. Bianchi. 2014. High frequency measurement of nitrate concentration in the Lower Mississippi River, USA. *Journal of Hydrology* 519:376-386.

Duncan, J. M., Welty, C., Kemper, J., Groffman, P. M., & L. E. Band. 2017. Dynamics of nitrate concentration-discharge patterns in an urban watershed. *Water Resources Research* 53:7349-7365.

Environmental Protection Agency. 2003. Nutrient and siltation TMDL development for Wissahickon Creek, Pennsylvania, Final Report, October 2003.

Figuerola-Nieves, D., McDowell, W. H., Potter, J. D., & G. Martínez. 2016. Limited uptake of nutrient input from sewage effluent in a tropical landscape. *Freshwater Science* 35(1):12-24.

Gammons, C. H., Babcock, J. N., Parker, S. R., & S. R. Poulson. 2011. Diel cycling and stable isotopes of dissolved oxygen, dissolved inorganic carbon, and nitrogenous species in a stream receiving treated municipal sewage. *Chemical Geology* 283:44-55.

Gibson, C. A. & J. L. Meyer. 2007. Nutrient uptake in a large urban river. *Journal of the American Water Resources Association* 43(3): 576-587.

Goyette, J. -O., Bennett, E. M., & R. Maranger. 2018. Low buffering capacity and slow recovery of anthropogenic phosphorus pollution in watersheds. *Nature Geoscience*.
doi:10.1038/s41561-018-0238-x.

Gücker, B., Brauns, M., & M. T. Pusch. 2006. Effects of wastewater treatment plant discharge on ecosystem structure and function of lowland streams. *Journal of the North American Benthological Society* 25(2):313-329.

Haggard, B. E., Storm, D. E., & E. H. Stanley. 2001. Effect of a point source input on stream nutrient retention. *Journal of the American Water Resources Association* 37(5): 1291-1299.

Haggard, B. E., Stanley, E. H., & D. E. Storm. 2005. Nutrient retention in a point-source enriched stream. *Journal of the North American Benthological Society* 24(1):29-47.

Hall Jr, R. O. & J. L. Tank. 2003. Ecosystem metabolism controls nitrogen uptake in streams in Grant Teton National Park, Wyoming. *Limnology and Oceanography* 48(3):1120-1128.

Halliday, S. J., Skeffington, R. A., Bowes, M. J., Gozzard, E., Newman, J. R., Loewenthal, M., ... & A. J. Wade. 2014. The water quality of the River Enborne, UK: Observations from high-frequency monitoring in a rural, lowland river system. *Water* 6:150-180.

doi:10.3390/w6010150.

Halliday, S. J., Skeffington, R. A., Wade, A. J., Bowes, M. J., Gozzard, E., Newman, J. R., ... & H. P. Jarvie. 2015. High-frequency water quality monitoring in an urban catchment: hydrochemical dynamics, primary production and implications for the Water Framework Directive. *Hydrological Processes* 29:3388-3407.

Heffernan, J. B. & M. J. Cohen. 2010. Direct and indirect coupling of primary production and diel nitrate dynamics in a subtropical spring-fed river. *Limnology and Oceanography* 55(2):677-688.

Hensley, R. T. & M. J. Cohen. 2016. On the emergence of diel solute signals in flowing waters. *Water Resources Research* 52:759-772. doi:10.1002/2015WR017895.

Jarvie, H. P., Neal, C., & Withers, P. J. 2006. Sewage-effluent phosphorus: a greater risk to river eutrophication than agricultural phosphorus? *Science of the Total Environment* 360(1-3):246-253.

Jones, C. S., Kim, S., Wilton, T. F., Schilling, K. E., & C. A. Davis. 2018. Nitrate uptake in an agricultural stream estimated from high-frequency, in-situ sensors. *Environmental Monitoring and Assessment* 190. doi:10.1007/s10661-018-6599-1.

Jordan, P., Arnscheidt, J., McGrogan, H., & S. McCormick. 2005. High-resolution phosphorus transfers at the catchment scale: the hidden importance of non-storm transfers. *Hydrology and Earth System Sciences* 9(6):685-691.

Koenig, L. E., Shattuck, M. D., Snyder, L. E., Potter, J. D., & W. H. McDowell. 2017. Deconstructing the effects of flow on DOC, nitrate, and major ion interactions using a high-frequency aquatic sensor network. *Water Resources Research* 53:10655-10673.

Martí, E., Aumatell, J., Gode, L., Poch, M., & F. Sabater. 2004. Nutrient retention efficiency in streams receiving inputs from wastewater treatment plants. *Journal of Environmental Quality* 33:285-293.

McDonnell, J. J. & K. Beven. 2014. Debates- the future of hydrological sciences: a (common) path forward? A call to action aimed at understanding velocities, celerities and residence time distributions of the headwater hydrograph. *Water Resources Research* 50(6):5342-5350.

Merseburger, G. C., Martí, E., & Sabater, F. 2005. Net changes in nutrient concentration below a point source input in two streams draining catchments with contrasting land use. *Science of the Total Environment* 347:217-229.

Mulholland, P. J., Marzolf, E. R., Webster, J. R., Hart, D. R., & Hendricks, S. P. 1997.

Evidence that hyporheic zones increase heterotrophic metabolism and phosphorus uptake in forested streams. *Limnology and Oceanography* 42(3):443-451.

Nimick, D. A., Gammons, C. H., & S. R. Parker. 2011. Diel biogeochemical processes and their effect on the aqueous chemistry of streams: a review. *Chemical Geology* 283:3-17.

Oelsner, G. P., Brooks, P. D., & J. F. Hogan. 2007. Nitrogen sources and sinks within the Middle Rio Grande, New Mexico. *Journal of the American Water Resources Association* 43(4): 850-863.

Pellerin, B. A., Downing, B. D., Kendall, C., Dahlgren, R. A., Kraus, T. E. C., Saraceno, J., ... & B. A. Bergamaschi. 2009. Assessing the sources and magnitude of diurnal nitrate variability in the San Joaquin River (California) with an in situ optical nitrate sensor and dual nitrate isotopes. *Freshwater Biology* 54:376-387.

Pellerin, B. A., Stauffer, B. A., Young, D. A., Sullivan, D. J., Bricker, S. B., Walbridge, M. R., ... & D. M. Shaw. 2016. Emerging tools for continuous nutrient monitoring networks: sensors advancing science and water resources protection. *Journal of the American Water Resources Association*. doi:10.1111/1752-1688.12386.

Philadelphia Water Department. 2007. Wissahickon Creek Watershed Comprehensive Characterization Report, available from:

http://www.phillywatersheds.org/doc/Wissahickon_CCR.pdf

Price, J. R., Ledford, S. H., Ryan, M. O., Toran, L., & C. M. Sales. 2018. Wastewater treatment plant effluent introduces recoverable shifts in microbial community composition in receiving streams. *Science of the Total Environment* 613-614:1104-1116.

Rahm, B. G., Hill, N. B., Shaw, S. B., & S. J. Riha. 2016. Nitrate dynamics in two streams impacted by wastewater treatment plant discharge: point sources or sinks? *Journal of the American Water Resources Association* 52(3): 592-604.

Ribot, M., Martí, E., von Schiller, D., Sabater, F., Daims, H., & T. J. Battin. 2012. Nitrogen processing and the role of epilithic biofilms downstream of a wastewater treatment plant. *Freshwater Science* 31(4):1057-1069.

Rode, M., Halbedel, S., Anis, M. R., Borchardt, D., & M. Weitere. 2016. Continuous in-stream assimilatory nitrate uptake from high-frequency sensor measurements. *Environmental Science & Technology* 50:5685-5694.

Ryan, R. J., Packman, A.I., & Kilham, S. S. 2007. Relating phosphorus uptake to changes in transient storage and streambed sediment characteristics in headwater tributaries of Valley Creek, an urbanizing watershed. *Journal of Hydrology* 336(3-4):444-457.

Scholefield, D., Le Goff, T., Braven, J., Ebdon, L., Long, T., & M. Butler. 2005. Concerted diurnal patterns in riverine nutrient concentrations and physical conditions. *Science of the Total Environment* 344:201-210.

Stream Solute Workshop. 1990. Concepts and methods for assessing solute dynamics in stream ecosystems. *Journal of the North American Benthological Society* 9(2):95-119.

Wade, A. J., Palmer-Felgate, E. J., Halliday, S. J., Skeffington, R. A., Loewenthal, M., Jarvie, H. P., ... & J. R. Newman. 2012. Hydrochemical processes in lowland rivers: insights from in situ high-resolution monitoring. *Hydrology and Earth System Sciences* 16:4323-4342.

Withers, P. J. A. & H. P. Jarvie. 2008. Delivery and cycling of phosphorus in rivers: a review. *Science of the Total Environment* 400: 379-395.

Wissahickon Valley Watershed Association (WVWA). 2017. Wissahickon watershed stream monitoring and assessment program: a summary of data collected by the Wissahickon Valley Watershed Association from 2004-2016. 92 pp.

Worrall, F., Howden, N. J. K., Burt, T. P., & R. Bartlett. 2019. The importance of sewage effluent discharge in the export of dissolved organic carbon from U.K. Rivers. *Hydrological Processes*. doi:10/1002/hyp.13442.

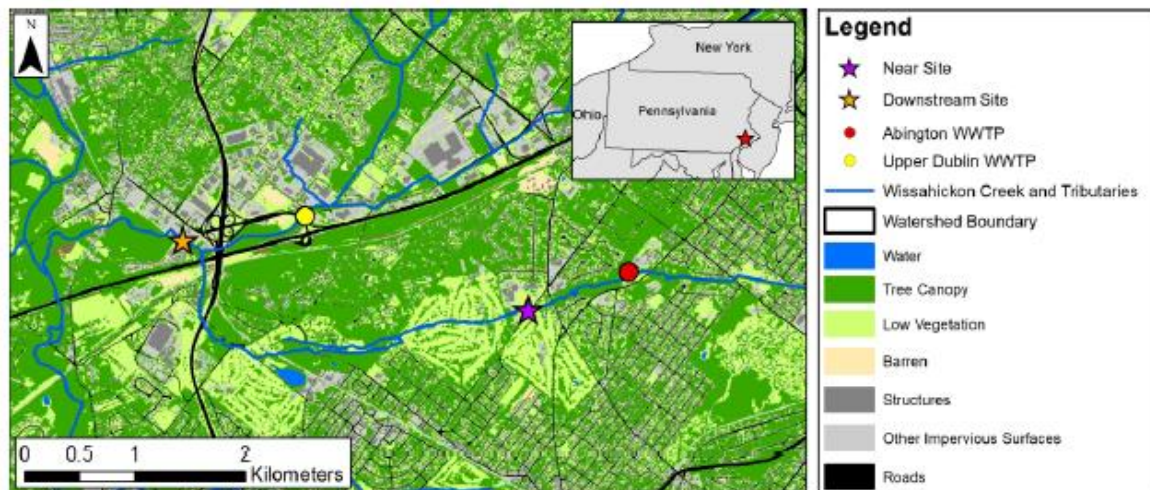


Fig. 1. Site map of sampling locations along Sandy Run, in Montgomery County, PA. WWTPs are identified with circles and locations of loggers are indicated with stars. Major land use in the area is low vegetation and trees, along with impervious surface cover including roads, structures, and parking lots.

Accepted Article

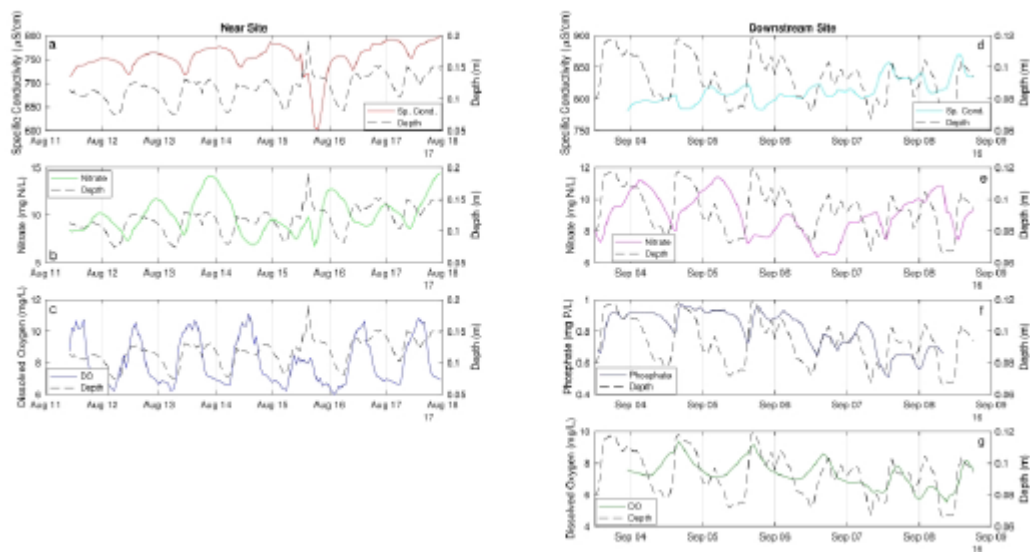


Fig. 2. a. Specific conductivity, in $\mu\text{S}/\text{cm}$, and depth, in m, through time at the near site; b. Nitrate, in mg N/L, and depth, in m, through time at the near site; c. Dissolved oxygen, in mg/L, and depth, in m, through time at the near site; d. Specific conductivity, in $\mu\text{S}/\text{cm}$, and depth, in m, through time at the downstream site; e. Nitrate, in mg N/L, and depth, in m, through time at the downstream site; f. Phosphate, in mg P/L, and depth, in m, through time at the downstream site; g. Dissolved oxygen, in mg/L, and depth, in m, through time at the near site. Vertical lines indicate midnight in all graphs.

Accepted

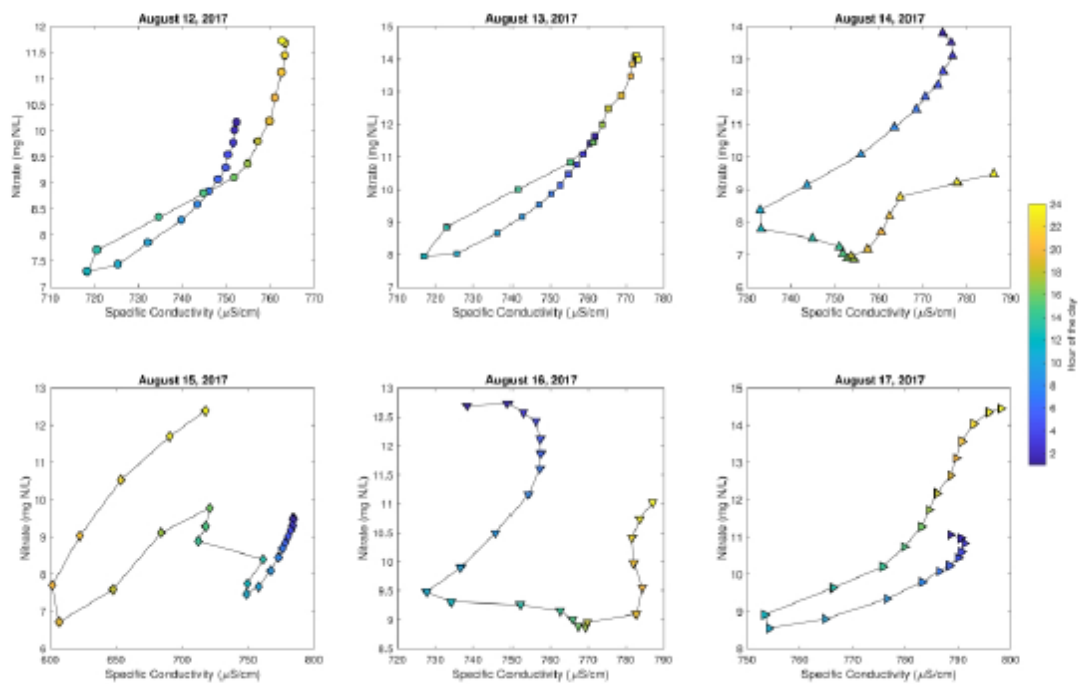


Fig 3. Specific conductivity, in $\mu\text{S}/\text{cm}$, vs. nitrate, in $\text{mg N}/\text{L}$, at the near site for each day. Hourly samples go from dark blue at midnight to yellow at 23:00. There was a small storm on August 15 and 16, 2017.

Accepted

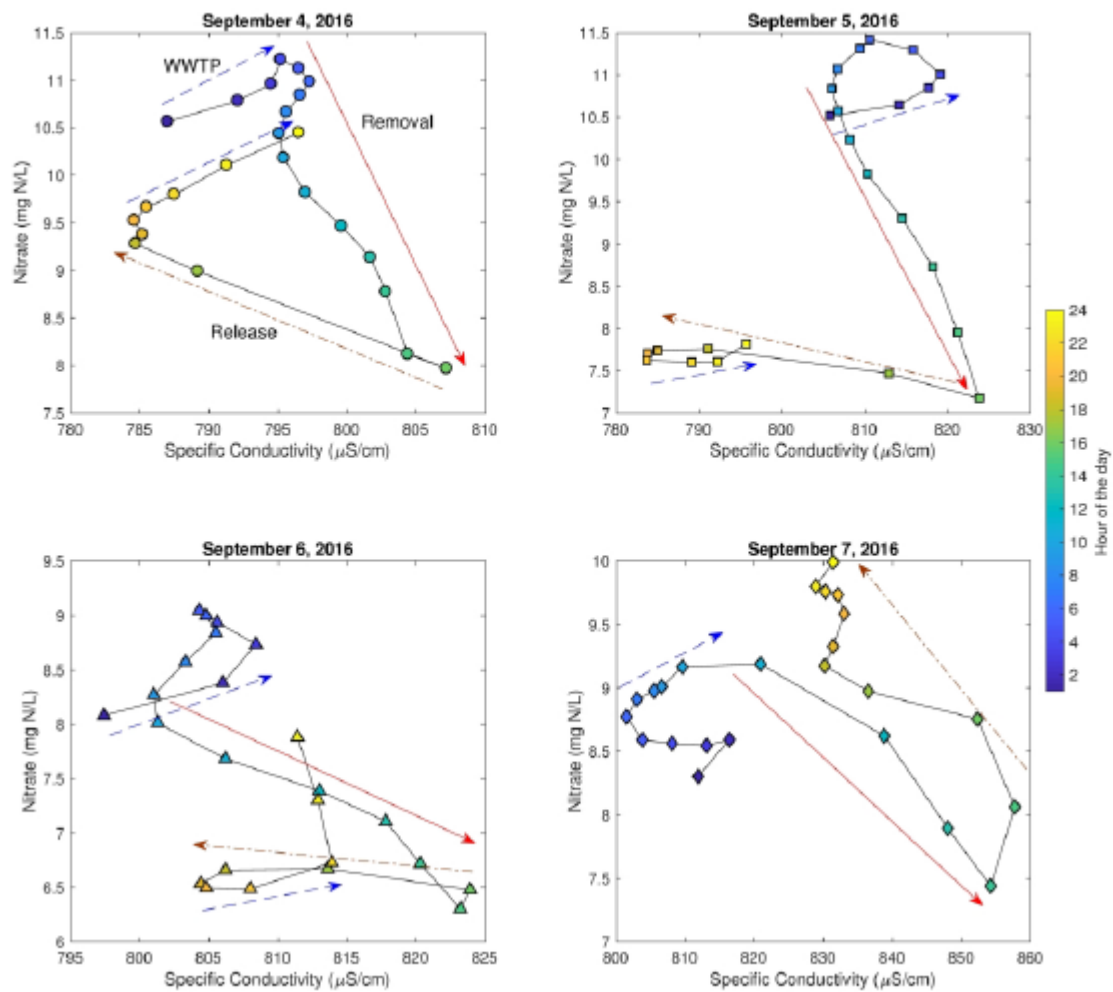


Fig. 4. Specific conductivity, in $\mu\text{S}/\text{cm}$, vs. nitrate, in mg N/L, at the downstream site for each day. Hourly samples go from dark blue at midnight to yellow at 23:00. Periods where the signal indicates WWTP source are shown in dashed blue arrows; periods where the signal indicates a removal process are shown in red arrows; periods where the signal indicates a release process are shown in dot-dash brown arrows.

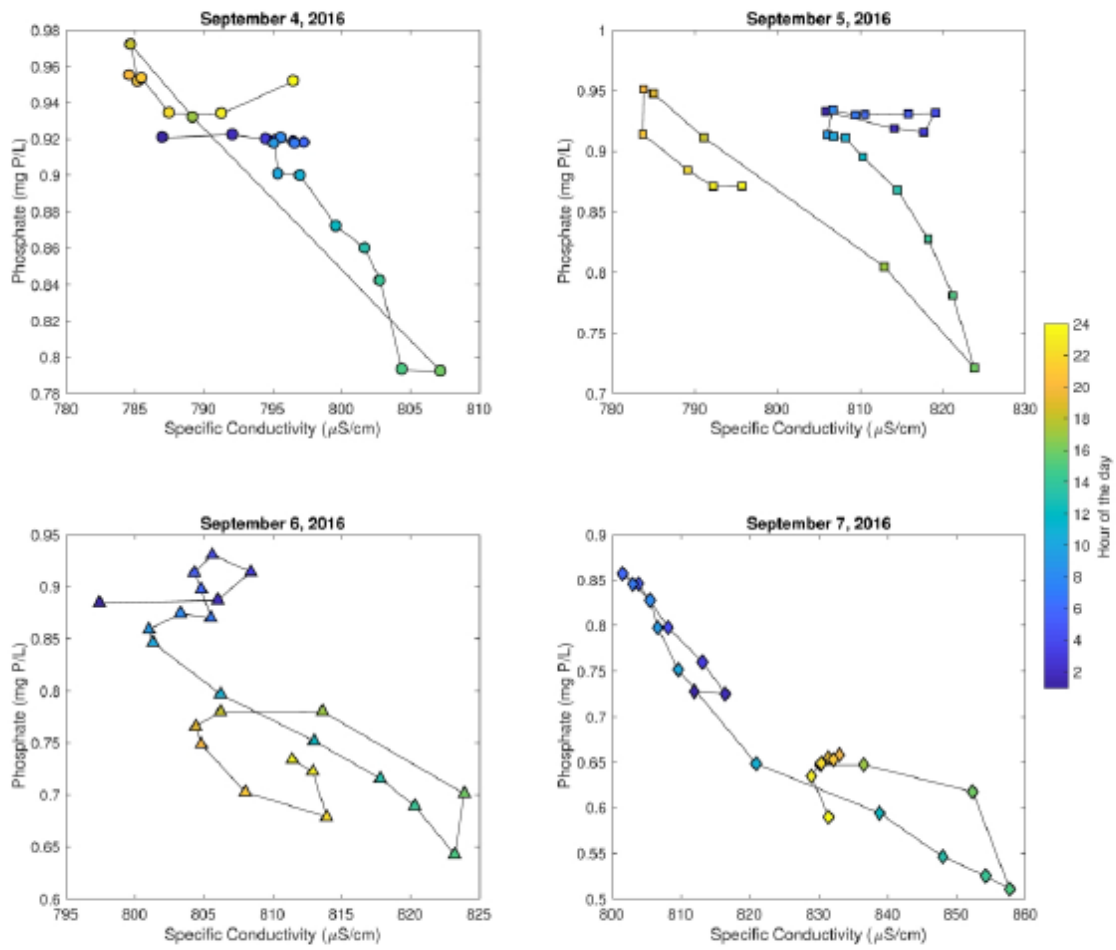


Fig. 5. Specific conductivity, in $\mu\text{S/cm}$, vs. orthophosphate, in mg P/L, at the downstream site. Hourly samples go from dark blue at midnight to yellow at 23:00.

Accept

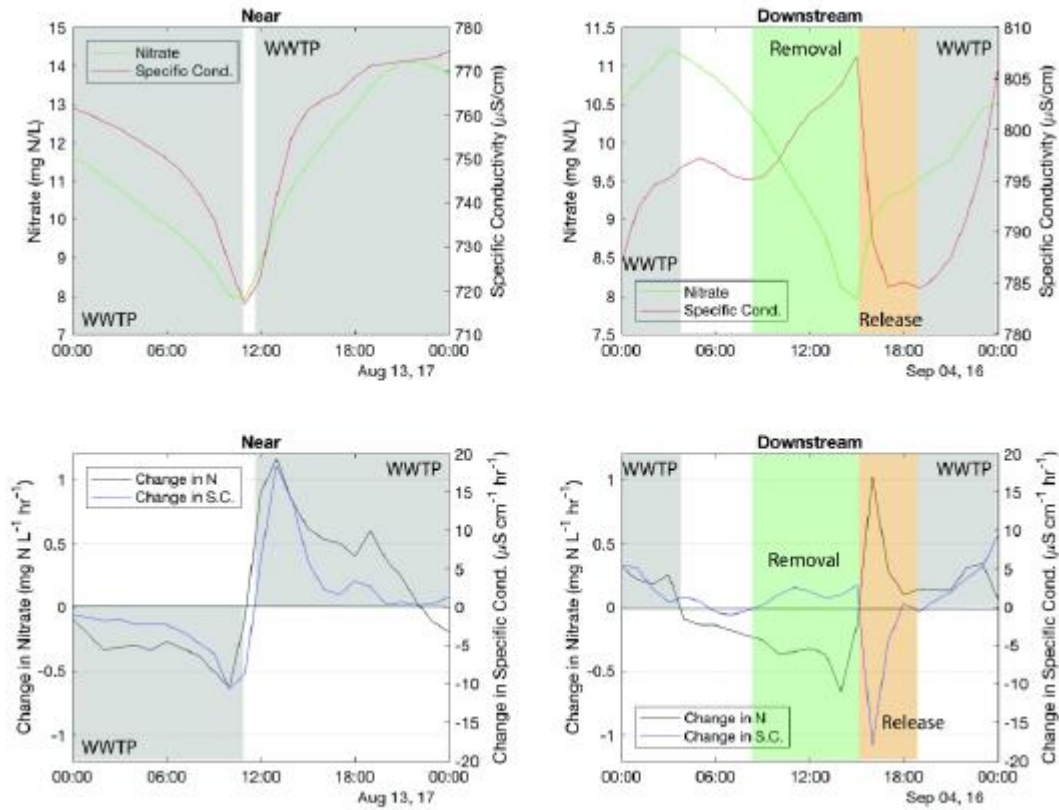


Fig. 6. Diagram of controls on in-stream nutrients. On the left is a single representative day from the near site and on the right is a single representative day from the downstream site. The top graphs are nitrate and specific conductivity through time. The lower graphs are hourly change in nitrate and specific conductivity through time. Times when specific conductivity and nitrate are changing together are indicative of downstream transport of the WWTP effluent signal, shown in grey boxes labeled “WWTP”. In the green box labeled “Removal”, nitrate is decreasing while specific conductivity increases, indicating removal of nitrate from the stream. In the orange box labeled “Release”, nitrate is increasing while specific conductivity decreases, indicating release of nitrate to the stream.

Table 1. Five most powerful frequencies for each time series, determined with Fast Fourier transformation, with frequencies listed from highest power to lowest. The highest power frequencies closest to 0.5 and 1 days are in italics, as they are related to WWTP signals and/or in-stream processing. Data are also shown in Fig. S3 and S5.

		Frequency (days)	Power
Near	Depth	<i>0.94</i>	3.6×10^{-6}
		1.10	3.4×10^{-6}
		<i>0.51</i>	2.5×10^{-6}
		1.32	1.8×10^{-6}
		0.47	1.1×10^{-6}
	Specific conductivity	3.33	4.9×10^{-3}
		2.17	4.0×10^{-3}
		<i>1.10</i>	4.0×10^{-3}
		1.32	3.5×10^{-3}
		0.82	3.5×10^{-3}
	Nitrate	<i>0.94</i>	2.9×10^{-4}
		2.17	2.9×10^{-4}
		1.10	2.6×10^{-4}
		3.33	2.4×10^{-4}
		0.82	2.0×10^{-4}
Downstream	Depth	<i>1.05</i>	3.8×10^{-6}
		<i>0.48</i>	2.9×10^{-6}
		0.88	1.4×10^{-6}
		0.75	1.0×10^{-6}
		0.58	1.0×10^{-6}
	Specific conductivity	<i>0.48</i>	3.6×10^{-3}
		<i>1.20</i>	3.3×10^{-3}
		0.81	2.1×10^{-3}
		4.76	1.7×10^{-3}
		0.97	1.6×10^{-3}
	Nitrate	<i>1.05</i>	3.3×10^{-4}
		5.26	2.9×10^{-4}
		2.63	2.8×10^{-4}
		1.32	1.4×10^{-4}
		0.88	1.2×10^{-4}
	Phosphate	4.76	2.4×10^{-5}
		<i>0.48</i>	1.9×10^{-5}
		<i>0.97</i>	1.8×10^{-5}
1.20		9.0×10^{-6}	
0.81		8.2×10^{-6}	

Table 2. In-stream metabolism modeling results from StreamMetabolizer for each site.

	GPP ($\text{g O}_2 \text{ m}^{-2} \text{ d}^{-1}$)	ER ($\text{g O}_2 \text{ m}^{-2} \text{ d}^{-1}$)	NEP ($\text{g O}_2 \text{ m}^{-2} \text{ d}^{-1}$)
--	------------------------------------------------------	-----------------------------------------------------	------------------------------------------------------

Near	3.9 (2.1 to 5.9)	-6.3 (-4.1 to -7.7)	-2.3 (-1.4 to -3.9)
Downstream	0.2 (0.1 to 0.3)	-0.7 (-0.5 to -0.8)	-0.4 (-0.3 to -0.6)

For all results, the first number is the average value over the days modeled and the range is reported in parentheses. Eight days were modeled near the plant and ten days were modeled downstream.

Accepted Article